Chapter 5

Influence of Substrate Wettability on Colloidal Assembly

Junchao Liu, Jingxia Wang and Lei Jiang

Additional information is available at the end of the chapter

http://dx.doi.org/10.5772/intechopen.71991

Abstract

In this paper, we presented a detailed discussion about the influence of the substrate wettability on the colloidal assembly and the resultant functionality of the films. It covers the basic assembly principle for colloidal crystals, the basic understanding of the substrate wettability on colloidal assembly, and the detailed explanation of the influence by give a full examples of various assembly from the substrate with distinct wettability, such as superhydrophilic, hydrophilic, hydrophobic, superhydrophobic and hydrophilic-hydrophobic pattern substrate.

Keywords: wettability of substrate, colloidal crystals, assembly

1. Introduction

Colloidal crystals [1–4] has aroused wide research attention owing to its fascinating light manipulation properties and important application in sensing [5–18], detecting [19–22], catalytic [23, 24] and some special optic devices [25–32]. Colloidal crystals are generally fabricated from the well-ordered assembly of the monodispersed latex particles or infiltrating the functional materials into the template and subsequent template removal (the typical fabrication process for the inverse opals). Accordingly, colloidal assembly plays an important role on the resultant functional, unique properties and the resulted potential applications. In this paper, we presented a detailed discussion about the influence of the substrate wettability on the colloidal assembly and the resultant functionality of the films. It covers the basic assembly principle for colloidal crystals, the basic understanding of the substrate wettability on colloidal assembly, and the detailed explanation of the influence by giving a full examples of various assembly from the substrate with distinct wettability, such as superhydrophilic, hydrophilic, hydrophobic, superhydrophobic and hydrophilic-hydrophobic pattern substrate.

2. Basic assembly principle for colloidal crystals

Colloidal assembly has become a well-known process since more than 5 decades' investigation of the colloidal assembly [33]. As shown in **Figure 1**, the colloidal assembly process includes the crystal nucleus by capillary force among latex particles, when the liquid front covers the half of the particles and crystal growth driven by the convective force owing to solvent evaporation and solvent reflux. A common mode for colloidal assembly includes vertical deposition approach. Where, the substrate is vertically placed in a colloidal solution, then a film of colloidal particles is formed at the interface between the substrate and the liquid surface with the solvent evaporation and the liquid surface drops. The formation of colloidal assembly is mainly originated from the driven force of capillary force between the drying colloidal particles at the meniscus of the solvent [34].

It is well known that the colloidal assembly is mainly depended on the assembly temperature, assembly humidity, and plenty of researches literatures took a careful investigation of the influence of various influencing factors on assembly behavior, assembly structure, and resultant property of colloidal crystals. Meantime, many assembly approach, such as spin coating, spray coating, inkjet printing, has been developed to improve the duplicated, assembly rate, controllable assembly, scalable assembly and high-quality assembly. Where, the vertical deposition approach has become a common method owing to its economic and easily duplicated in most laboratory (**Figure 1C**). In this following part, we would like to discuss the influence of the substrate wettability on colloidal assembly.

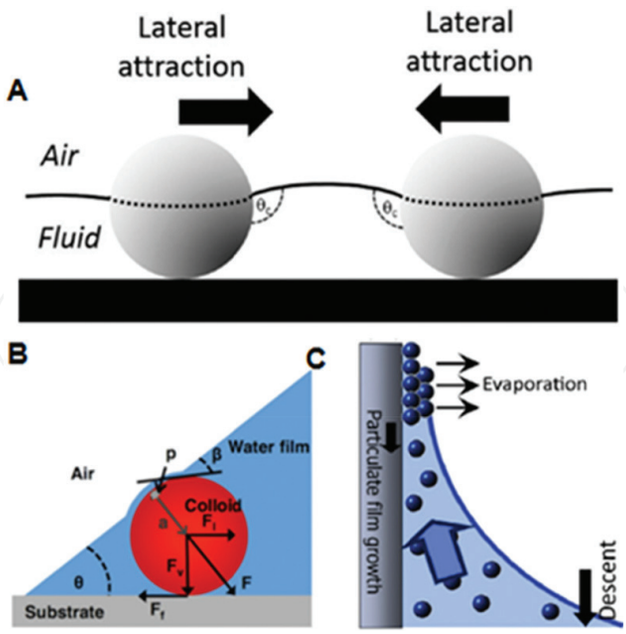

Figure 1. Mechanism of colloidal PCs assembly. (A) Colloidal particles assembly forced by the liquid flow as evaporation of the solvent; (B) acting on a colloid trapped at an air water substrate interface; (C) schematic illustration of the convective self-assembly technique in vertical deposition way [33, 34].

http://dx.doi.org/10.5772/intechopen.71991

3. Basic understanding of the substrate's wettability on colloidal assembly

To understand the basic influence of the wettability on colloidal assembly, we present a basic concept of the substrate wettability and depict a detailed analysis about the effect of substrate wettability on the assembly process, assembly force and etc.

3.1. Basic concept of substrate wettability and the basic understanding of the wettability on the colloidal assembly

Wettability is a basic property of liquid on solid surface, it is determined by surface chemical composition and surface roughness, as shown in **Figure 2**. Generally, the wettability is evaluated by the water contact angle (CA), i.e., static CA. It is defined by integrated angle for the three-phase contact line of liquid, gas and solid after a droplet spread on the substrate (**Figure 2A**). Based on different statistic CA, distinct substrate is determined. The hydrophilic substrate with CA < 65°, indicating a strong attraction of liquid on solid surface, which results in droplet spreading. Especially superhydrophilic substrate is obtained when CA is around 0° (**Figure 2C**). Hydrophobic substrate with CA > 90°, meaning a limited attraction between solid and liquid surface, a less spread is observed for droplet on the substrate. Recently, the diving line is set as 65°, a new dividing line

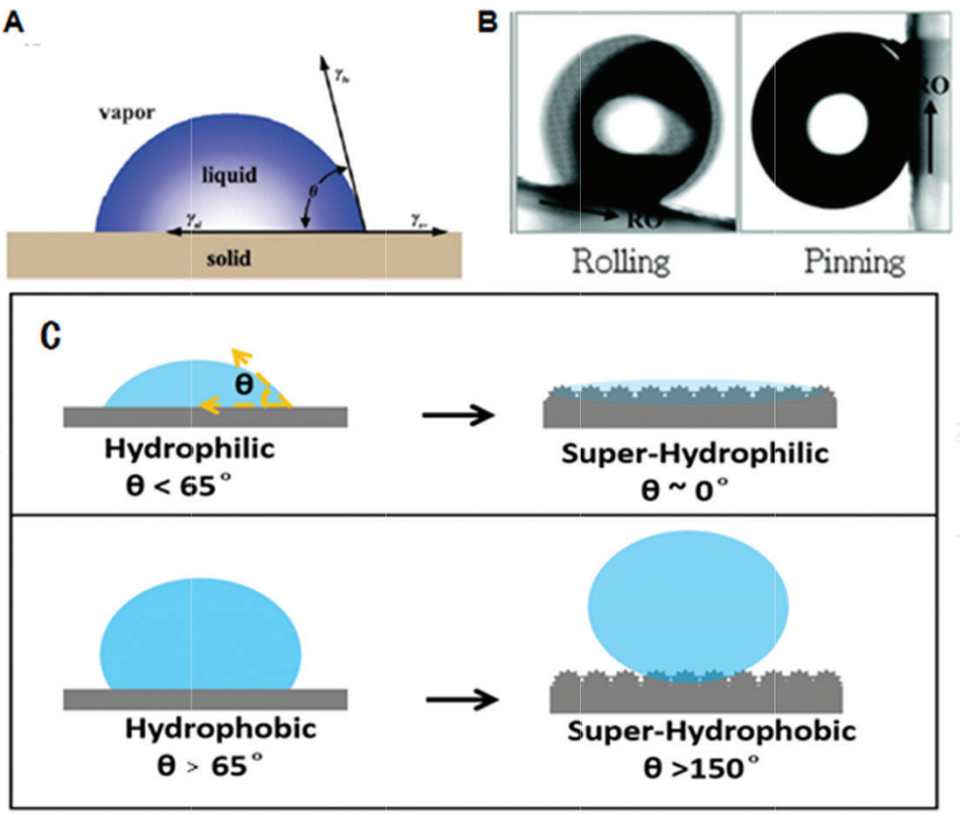

Figure 2. Wettability of interfaces. (A) Statistic contact angle, (B) sliding angle with different substrate adhesive, (C) schematic illustration of different wettability state [35].

between hydrophilic and hydrophobic, is defined by Prof. Lei Jiang. Superhydrophobic substrate with water CA > 150°, is a special substrate, it is difficult for the droplet to spread upon it. Such as the lotus surface. Besides statistic CA, sliding angle is also a judgment of wettability of substrate. As shown in **Figure 2B**, when a droplet and three phase contact line (TCL) can stay steadily on a solid substrate it indicates high-adhesive, in the contrast, droplet and TCL can easily move on a low-adhesive substrate. Both static CA and the sliding angle plays an important role on the colloidal assembly. The substrate with different water CA showed various potential applications.

3.2. Basic understanding of the influence of the substrate wettability on colloidal assembly from static and dynamic wettability

Here, we understand the influence of the substrate's wettability on colloidal assembly by qualitatively analyzing the relationship between the substrate wettability on the evaporation time/rate and the evaporation force when a droplet spreading on the substrate. As shown in **Figure 3**, for the hydrophilic substrate with lower CA, having a large spreading area. In this

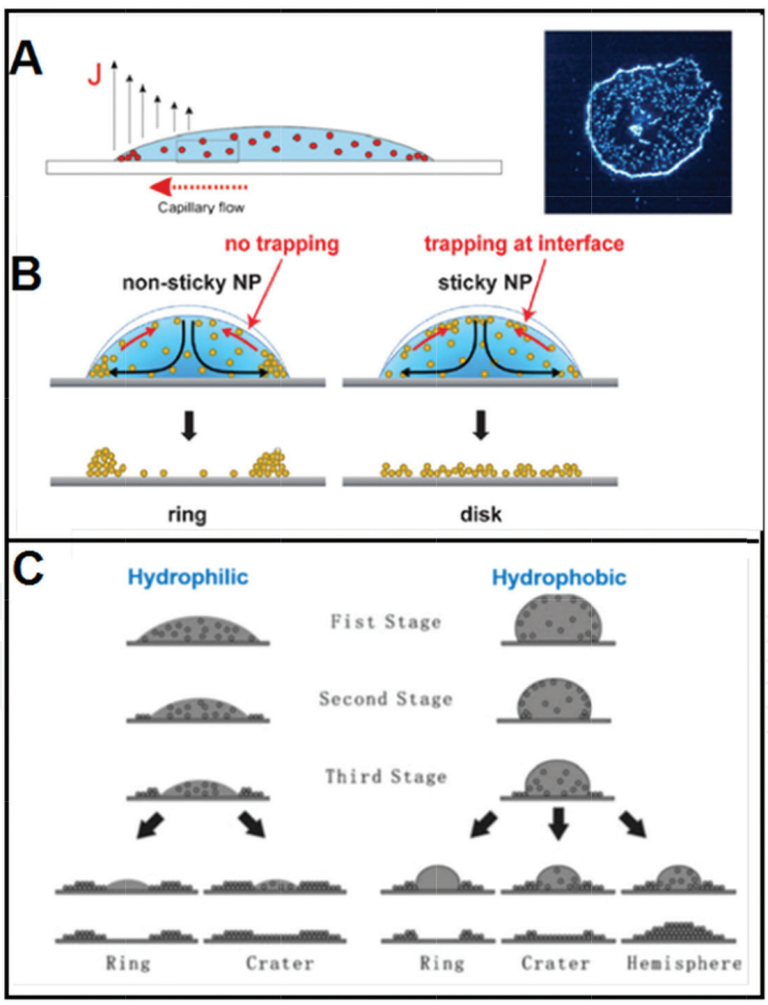

Figure 3. Formation of colloidal PCs as substrate is hydrophilic. (A) Illustration of coffee stain formation and a microscope image of a coffee stain formed by fluorescently labeled 5-μm particles; (B) on a hydrophilic substrate, the competition of Marangoni flow (red arrows) and the evaporation-driven capillary flow (black arrows) resulted the ring-shape or the disk shape. (C) Schematic depiction of the aggregation of monodisperse spheres on hydrophilic PMMA and hydrophobic FAS-coated glass substrates [36].

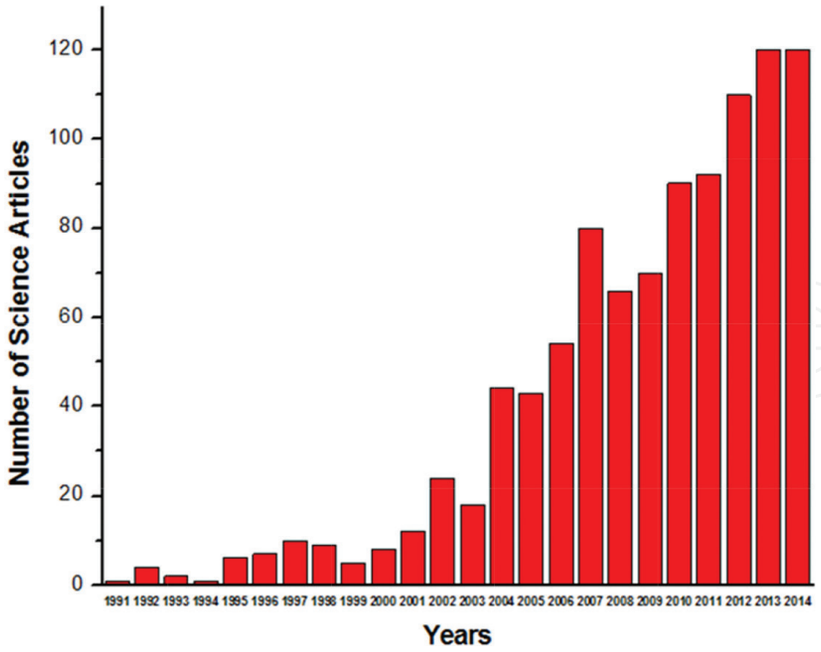

Figure 4. Number of science articles that searching result of "assembly" + "wettability".

case, the droplet keeps constant contact area and decreased water CA during evaporation process, as a result, a short time or fast evaporation rate is observed for the droplet evaporation. In contrast, when droplet is on the hydrophobic substrate, the droplet keeps constant CA but a decreased contact area during evaporation process. As a result, a longer evaporation time and slower evaporation rate occurs in the evaporation system. Accordingly, there would be a short assembly time on hydrophilic substrate, and a longer assembly time on hydrophobic substrate. On the other hand, substrate wettability will affects the pinning or sliding or TCL on the substrate, the sliding TCL will produce an addition driven force for the latex assembly, will contributing to distinct assembly structure and colloidal property as well.

As regarding of the research progress related to the influence of the wettability on colloidal assembly, there is an obvious increased paper published after Year 2004, as shown in **Figure 4**. Which presented the research papers number (related to colloidal assembly & wettability) ranging from 1991 to 2014, the data is searched from database of Web of Science. Clearly, less papers is related to the colloidal assembly &wettability prior to 2004, there are only 1–2 papers published in 1991. In comparison, a rapid growth of the paper numbers related to colloidal assembly/wettability occurred after the period. More than 100 papers published related to the topic in Year 2014. In the following part, we will list a full example to understand what the influence of the substrate's wettability on the colloidal assembly.

4. Full examples for the understanding of the influence of wettability on colloidal assembly

Wettability of substrate plays an important effect on the colloidal assembly by affecting its assembly time, assembly rate and assembly process. In this section, we summarized various

examples to give a full description of the influence of the wettability on the colloidal assembly process and its resultant assembly structure. Wherein, the substrate with wettability, such as superhydrophilic, hydrophilic, hydrophobic, superhydrophobic, pattern-substrate is considered.

4.1. Superhydrophilic substrate

Superhydrophilic substrate with water CA of 0°, shows excellent spreading behavior for the colloidal suspension. In this case, the resultant colloidal assembly structure showed an uniform distribution. Therefore, superhydrophilic substrate is generally thought to be optimal substrate for the colloidal assembly at the earlier assembly literature. How to achieve a superhydrophilic substrate has ever to be an important technical issue for the well-ordered colloidal assembly [37]. Accordingly, many early assembled literatures are carried out on superhydrophilic substrate. Many outstanding and impressing assembly work is done on superhydrophilic substrate. Typically, many colloidal crystals are assembled on superhydrophilic substrate by vertical deposition, spin coating, spray coating.

4.2. Hydrophilic substrate

Hydrophilic substrate with water CA <65° have a special "coffee-ring" effect on colloidal assembly. Coffee ring is aroused owing to the faster evaporation rate in the exterior region of the droplet comparing that interior region, thus more latex transfer from the interior toward the exterior region, which resulted in the more deposit and assembly of the latex particles at the brim of the droplet, leaving less latex at the center of the droplet, forming a ring-shaped structure (left part of **Figure 3B** and **C**). Much work is developed to remove coffee ring effect by introducing temperature filed, surfactant. Of course, some researchers fabricated some interesting pattern by taking advantage of the coffee-ring effect. For example, Gu et al. [36] displayed different assemble modes of PC in hydrophilic and hydrophobic substrate in **Figure 3**. They used different concentration suspension dripple onto polymethyl methacrylate (PMMA) substrate and FAS-treated glass substrate in the hydrophilic substrate, ring and crater structure can be obtained, while on hydrophobic substrate, hemisphere structure also appear for the liquid shrink to a dot. The assembly process of colloidal particles on different wettability substrate can be described as follows. Furthermore, Gu et al. developed a ring-shape colloidal crystal by taking advantage of coffee-ring phenomenon for artificial eye-pupil structure.

4.3. Hydrophobic substrate

Hydrophobic substrate with water CA of higher than 65°, showed special evaporation behavior than that on the hydrophilic substrate. Particularly, TCL recedes owing to the lower adhesive force of particles on the substrate when droplet evaporating on hydrophobic substrate. Just because the receding TCL, the coffee ring effect can be effectively removed on hydrophobic substrate (right part in **Figure 3B** and **C**). In this case, a sphere-rich phase near the solvent/air interface was caused by evaporation of the solvent (first stage); the crystallization of spheres at the rim of drop occurred when the concentration exceeded a critical value (second

stage); receding TCL aggregate the latex toward the center of the droplet (third stage). As a result, a final compact assembly structure can be obtained "similar to dome". The application of the hydrophobic substrate may produce some novel and functional assembly structure.

Liu et al. [38] fabricated controllable inkjet printing lines by adjusting the ink droplets' dynamic wettability on hydrophobic substrate (**Figure 5A** and **B**). Mixing the ink with water and ethylene glycol to adjust the ink droplet's surface tension and the nanoparticle concentration. Distinct dynamic wettability of ink droplets on the hydrophobic substrate could be achieved owing to the different surface tension and nanoparticle concentration. In the first case, the surface tension of droplet 1 and 2 were similar, the TCL of droplet was hardly pinned owing to no particle assembly at TCL. A spherical cap was obtained after coalescing and drying of ink, as shown in **Figure 5A**$_1$. In contrast, if the surface tension of droplet 1 was smaller than droplet 2, the TCL of droplet was pinned and a straight line could be obtained after coalescing and drying owing to nanoparticles assembled at the TCL of the droplet 1. Furthermore, a stronger pinning TCL and dumbbell shape was formed with more nanoparticles assembling at the TCL, as shown in **Figure 5A**$_2$ and **A**$_3$. As a result, different line shapes of wave, straight footprint and wave with straight footprint were obtained, as shown in **Figure 5B**. Hydrophobic substrate was used for the removal of the coffee ring. Typically, Cui et al. [40] made a research about a drop of a colloidal suspension of latex spheres dropped onto a hydrophobic-silica pillar array (HSPA) with high contact hysteresis to remove coffee ring effect. In details, a drop of colloidal suspension with latex spheres presents a Wenzel state with high CA hysteresis on the surface of HSPA, which leads to the pinning of contact line (CL) during the solvent evaporation. Then more latex spheres will be deposited on the periphery of the drop to accelerate growth of the porous gel foot (means the aggregation of latex spheres at the edge of the droplet). Subsequently, the capillary

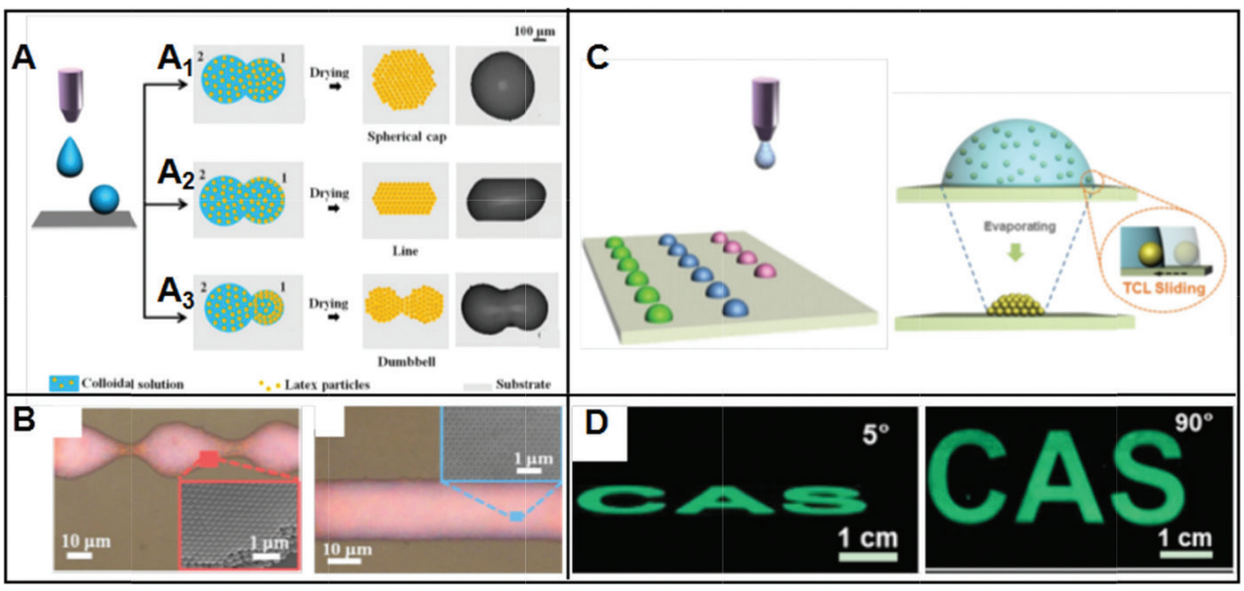

Figure 5. (A) Three typical coalescing cases of the neighboring ink droplets induced by different dynamic wettability of ink droplets on the substrates. (B) Optical microscope images of the as-printed PC lines with wave and straight footprints. Three typical straight PC lines (red, green, and blue) demonstrating good optical properties and the insets are the corresponding SEM images [38]. (C, D) fabrication of photonic crystal dome on hydrophobic substrate by inkjet printing [39].

flow formed based on a growing gel foot. Finally, a uniform colloidal deposition without a coffee ring structure is obtained owing to the existence of gel foot and capillary flow. Finally, "coffee ring" diminished as well as closed-packing PC structure can be obtained. Due to the fast shrinking of the TPCL. Furthermore, hydrophobic substrate was used for the fabricated of the PC dome array by inkjet printing by Kuang et al. [39] in **Figure 5C–D**. They inkjet printed latex suspension on the hydrophobic substrate, obtained dome-like PC sphere, which can effectively avoid the angle-dependent property of the stopband of PC, providing an important insight for the wide-view display applications of PCs. That is, the hydrophobic substrate provides an effective approach for the fabrication of colloidal crystals with excellent wide-angle property [41–46].

4.4. Superhydrophobic substrate

Superhydrophobic substrate is a special substrate with water CA > 150°, the rolling angle less than 5°, as well as low adhesive surface. The large water CA makes it possible for the spherical colloidal assembly. While the low-adhesive property of substrate contributed to the formation of crack-free colloidal assembly.

The application of superhydrophobic substrate is helpful for the fabrication of spherical PCs and crack-free colloidal PCs. For example, Velev et al. [47] reported an approach for colloidal assembly in droplets on superhydrophobic substrates (**Figure 6A**), which yields

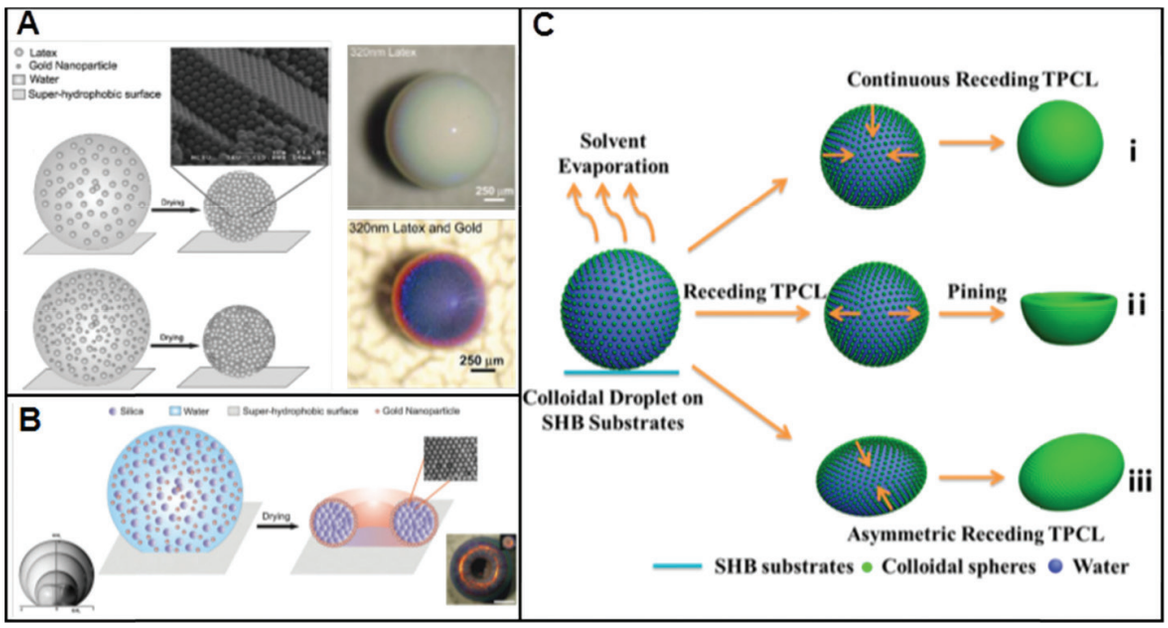

Figure 6. (A) Schematics of the process for making spherical colloidal assemblies on superhydrophobic. The inset displays the hexagonal close-packed structure of latex spheres inside an opal ball of 540 nm latex [47]. (B) Schematic of supra-particle formation by evaporating a droplet containing suspension of silica and gold nanoparticles. Top and angled view of "golden doughnut" supra-particles on the right-down inset. The inset on the left-down shows an overlay of experimental images for the side-view profile of a drying droplet with silica particles over time fabricated from a droplet containing 330-nm-diameter silica [48]. (C) Schematic illustrations of the microshape fabrication of PC particles on superhydrophobic substrates based on different dynamic behaviors of the TCL, (i) continuous receding, (ii) receding and then pinning, and (iii) asymmetric receding of the TCL [49].

better control over the final shape and creates supra-particles that are easily detached and ready to use. The resultant colloidal assembly is near-spherical and spheroidal supraballs. The process of sample are as follows: the droplet of colloidal latex or mixed with gold nanoparticles showed superhydrophobic and high CA hysteresis owing to the small pinning areas formed between low-density polyethylene and substrate. Thus the colloidal spheres were inclined to form a close-packed microsphere crystals with the evaporation of solvents due to the decrease of free volume between latex particles. As a result, the spherical colloidal PC with colored ringlike diffraction patterns was formed. Later, they developed this method and obtained shape-anisotropic ("doughnut") and composition-anisotropic ("patchy magnetic") supra-particles [48] in **Figure 6B**. At the initial stage, near-spherical shape was obtained due to a high contact angle. During the process of solvent evaporation, silica suspension droplets undergo shape transitions (concaving) leading the structure of the final assemblies to doughnut supra-particles. Furthermore, composition anisotropy is achieved by drying a droplet containing a mixed suspension of latex and magnetic nanoparticles among a magnetic field gradients. The magnetic nanoparticles assembled into single, bilateral, or trilateral, patched spherical supra-particles. Additionally, the shape of the microsphere can be tuned by Zhou et al. from microbeads to microwells to microellipsoids via adjusting the dynamic behaviors of the three-phase contact line (TCL) during the evaporating process on superhydrophobic substrates [49] (**Figure 6C**). The assembly of PC structure is prepared by dispensing aqueous colloidal latex spheres droplet (acting as self-assembly template) onto superhydrophobic substrate and evaporates naturally. The high CA (≈151°) of colloidal latex droplet on the superhydrophobic substrate contributed to the formation of self-assemblies templates. Microbead PC assemblies was obtained by continuous homogeneous receding of the TCL of the aqueous colloidal droplet evaporating on superhydrophobic substrate (scheme C_i). But for dimpled microbead or microwell PC assemblies (scheme C_{ii}), the reason for its formation maybe the change in the moving directions of the colloidal spheres caused by pinning of the TCL during aqueous colloidal droplet evaporation. Furthermore, asymmetric receding of TCL benefits the interesting anisotropic PC assemblies (scheme C_{iii}). It worth to be noted that high-quality crack-free colloidal PC can be fabricated from superhydrophobic substrate. For instance, Huang et al. [50] fabricated a centimeter scale PCs on low-adhesive super-hydrophobic substrates (**Figure 7**). It shows the schematic illustration of colloidal PCs assembled on high F_{ad} substrate and low F_{ad} superhydrophobic substrate. The red dashed lines indicate the changing trend of the TCL during different drying conditions. The latex particles at first assemble on the surface of the suspension, and then shrink with further solvent evaporation. When the latex particles dry on a substrate with high F_{ad}, the pinned TCL and latex shrinkage causes tensile stress and crack formation. In contrast, large-scale crack-free colloidal PCs are achieved on a superhydrophobic substrate with low F_{ad} due to the timely release of tensile stress as the TCL recedes. The sample showed high quality and crack-free property, it is especially important, the sample showed an evident narrow stopband with full-width-at-half-maxima of the stopbands of just 12 nm due to the receding TCL during evaporation process, which releases the tensile stress induced by latex shrinkage. The work is of great significance for the creation of novel and high-quality PC optic devices.

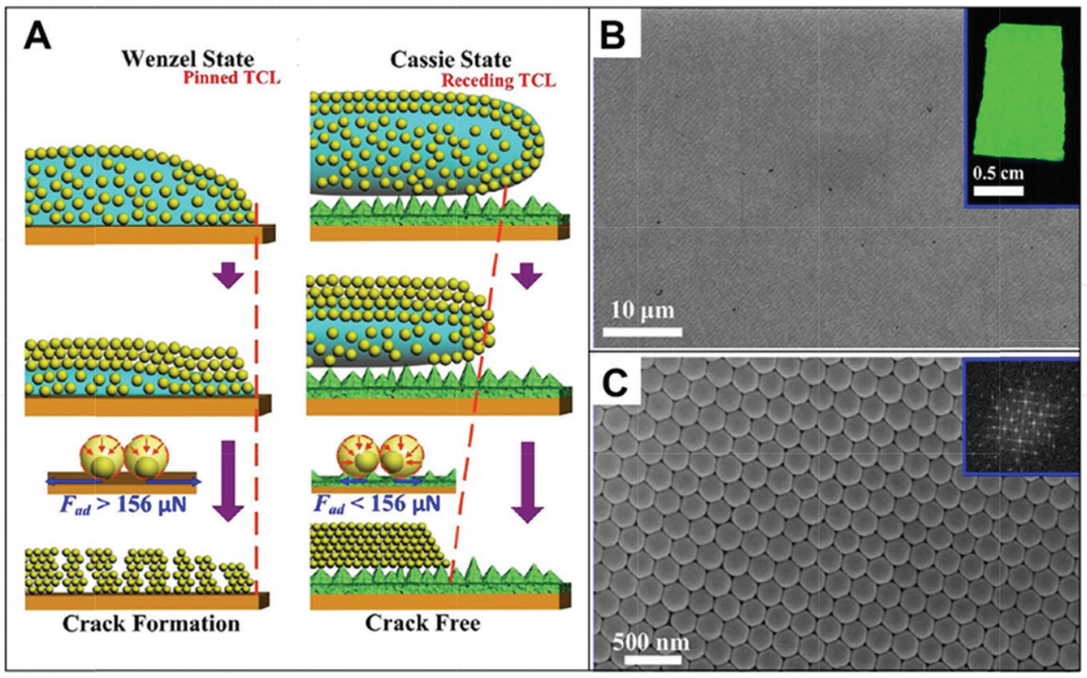

Figure 7. (A) Schematic illustration for the fabrication of crack-free PC on low-adhesive superhydrophobic substrate. (B, C) SEM images of the as-prepared colloidal PCs with diameter of 224 nm assembled on low-adhesive superhydrophobic substrate. The images demonstrate perfectly ordered latex arrangement and close-packed assembly structures of the PCs [50].

4.5. Pattern colloidal crystals from the combination of the hydrophilic/hydrophobic substrate

Wettability also can be used for design patterned PCs [51]. Colloidal crystals with different patterns in various colors may be obtained through tuning the wettability of assemble substrate, and different particles, Also, asymmetric or dissymmetric pattern can also be created in wettability gradient surface.

Figure 8A exhibited a detailed description about the fabrication of the substrate with modified wettability. For example, Young et al. demonstrated the structure of the PS colloidal crystals which were fabricated on the hydrophilic/hydrophobic Si wafers by a spin-coating technique (**Figure 8A)**. PS spheres organized as ordered close-packed face-centered cubic structure on the hydrophilic surface while they gathered without the crystal structure on the hydrophobic surface. Lee et al. [52] made site-selective assembly available and designed a surface with alternating wetting region and dewetting region in **Figure 8B**, then the particles only confined and assembled in the wet region. Therefore, wettability induced PC pattern can be obtained. The basic concept of site-selective assembly of colloidal particles on a wettability-patterned surface are shown in **Figure 8B**. The relative fraction of the wet region W to the dewet region D and droplet volume decided the wetting layer morphology including the CA. First, a generate patterned wettability was obtained by liquid crystal (LC) alignment layer irradiated via UV light through a photomask. Then a periodic array of circular W regions surrounded by intact D regions was obtained. When dropping an LC/prepolymer solution with colloidal particles on the as-prepared wettability patterned substrate, it could

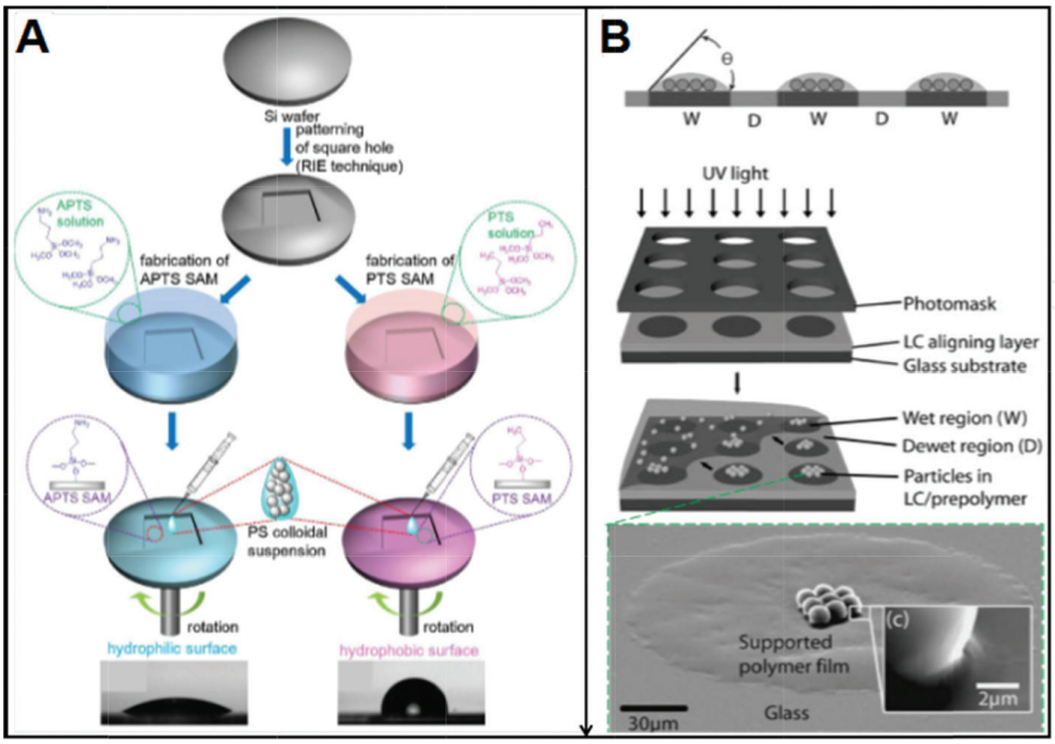

Figure 8. (A) a detailed description about the fabrication of the substrate with modified wettability. (B) schematic diagrams showing underlying concept of site-selective assembly of colloidal particles: Liquid crystal (LC)/prepolymer solution containing colloidal particles on wettability-patterned surface with wet regions (W) and dewet regions (D) and wettability-patterning process using UV exposure on LC alignment layer (top) and array of LC/prepolymer droplets produced only in wet regions where the colloidal particles are confined (bottom) [52].

be confined to the W regions. A highly close-packed structure of colloidal particles located in the W region was formed. Trough different value of H, two assembly cases of colloidal particles that in central or boundary regions could be formed.

Wu et al. [53] presented a strategy to fabricate controllable 3D structures and morphologies from one single droplet via inkjet printing (**Figure 9A** and **B**). The 3D morphology of microcolloidal crystal pattern was controlled by hydrophilic pattern induced asymmetric dewetting. First, using a hydrophobic silicon wafer with patterned hydrophilic pinning spots (green shading) as substrate. Then nanoparticles contained precisely designed droplets array was prepared by inkjet printing. Arrayed 3D microcolloidal crystals with controllable morphology were achieved owing to the hydrophilic pattern induced asymmetric dewetting. Many morphologies of quadrilateral, pentagon, hexagon and etc. could be obtained through different hydrophilic patterns. Wang et al. [54] fabricated a microring PC made of colloidal particles by taking advantage of a superhydrophilic flat transfer substrate and a superhydrophobic groove–structured silicon template (**Figure 9C**). The process of "sandwich assembly" was mainly used by a superhydrophobic groove structured template and a flat superhydrophilic transfer substrate. The as-prepared microrings showed homogeneous bring–green color owing to the fluorescent signal and favorable waveguide property. Yoo et al. [55] reported a flexible superhydrophobic PDMS cage formed by superhydrophobic patterns encompassing the unmodified region for aqueous

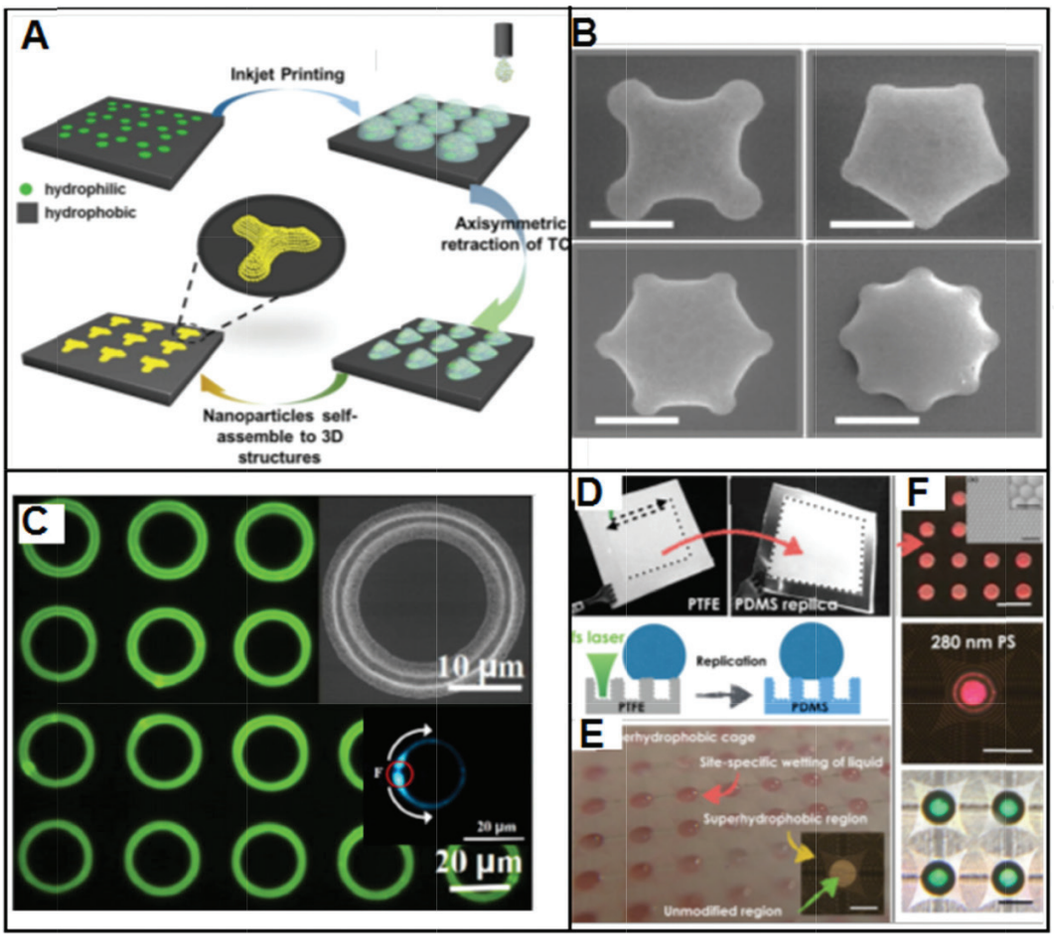

Figure 9. (A) Manipulating 3D morphology of microcolloidal crystal pattern through hydrophilic pattern induced asymmetric dewetting. (B) SEM images of various assembly units through designed hydrophilic pinning pattern [53]. (C) Fluorescence optical and SEM images of micro-ring PC and its waveguide property [54]. (D) Schematics of superhydrophobic surface production by FS laser direct writing. Photographs of superhydrophobic polytetrafluoroethylene (PTFE) film and superhydrophobic polydimethylsiloxane (PDMS) replica. (E) PDMS superhydrophobic cage. (F) Microscopic pictures of self-assembled structures on a superhydrophobic cage. The scale bars are 1 mm. Magnified reflection and transmission microscopic pictures of self-assembled structures consisting of 280 nm PS particles from colloidal droplets. Scale bars are 500 μm [55].

droplet positioning and trapping in **Figure 9D**. A PTFE film with nano-sized bumpy structures could be fabricated by femtosecond laser ablation under ambient conditions. Then a superhydrophobic PDMS surface was easily replicated from the superhydrophobic PTFE mold owing to the tribological properties of PTFE. As a result, a superhydrophobic cage structure on a PDMS replica surface was prepared by laser enabled direct writing. The optical image of one superhydrophobic cage structure was shown in **Figure 9D**. Subsequently, dropping a liquid with colloidal particles on the surface of superhydrophobic PDMS, colloidal particles self-assembly in this superhydrophobic cage during evaporation process, forming a self-assembled PC.

Choi et al. [44] employed a fast, high-through method to fabricate size-tunable micro/nanoparticle clusters via evaporative assembly in picoliter-scale droplets of particle suspension on hydrophobic substrate. Various morphologies that particle clusters with accurate positioning

and alignment are demonstrated (shown in **Figure 10A** and **B**). the whole fabrication process includes: (i) Particle suspension menisci are extruded to the upfront end of the membrane by gravity. (ii) Contact of the head with the substrate is achieved. (iii) Surface tension of the substrate attracts a fraction of the suspension fluid. (iv) Picoliter-scale droplets are transferred to the substrate via pinch-off processes. (v) Rapid evaporative self-assembly of the particles forms 3-D clusters. In this case, the printing head was fabricated by the method of applying traditional microfabrication technology to SOI (Silicon-On-Insulator) substrates while a micro/nanoparticle suspension container was achieved by being wet-etched of backside. A microporous membrane with a 200 nm thickness was released on the head after the above whole process. After the suspension was loaded into the head, the meniscus of the droplet was completely extruded to the front of the head. Then, multiple picoliter-scale (2 − 20pL) droplet of particle suspension was transferred from the bulk suspension to the substrate by direct contact of the head with the substrate. This whole process could be achieved less than 5 s. The evaporative self-assembly process is controlled by gravity force and surface tension force of a contacting surface and controlled sizes and spacing of particle clusters.

Kim et al. [56] reported a novel and controllable patterning technique for 3D or 2D colloidal arrays of polymeric domes using photocurable emulsion droplets as templates (**Figure 10C–E**). The oil-in-water emulsion droplets will adhere selectively on the surface with a high interfacial affinity. The preparation process includes the following parts: first, a patterned glass substrate was prepared by microcontact printing with a hydrophobic ink of octadecyltrichlorosilane (OST). The OTS molecules binded covalently on the clean glass which from a poly(dimethylsiloxane) (PDMS) stamp. PDMS stamps had cylindrical posts of patterned arrays or characters by soft-lithography. Then, dropping oil-in-water emulsion in the surface of prepatterned glass substrate.

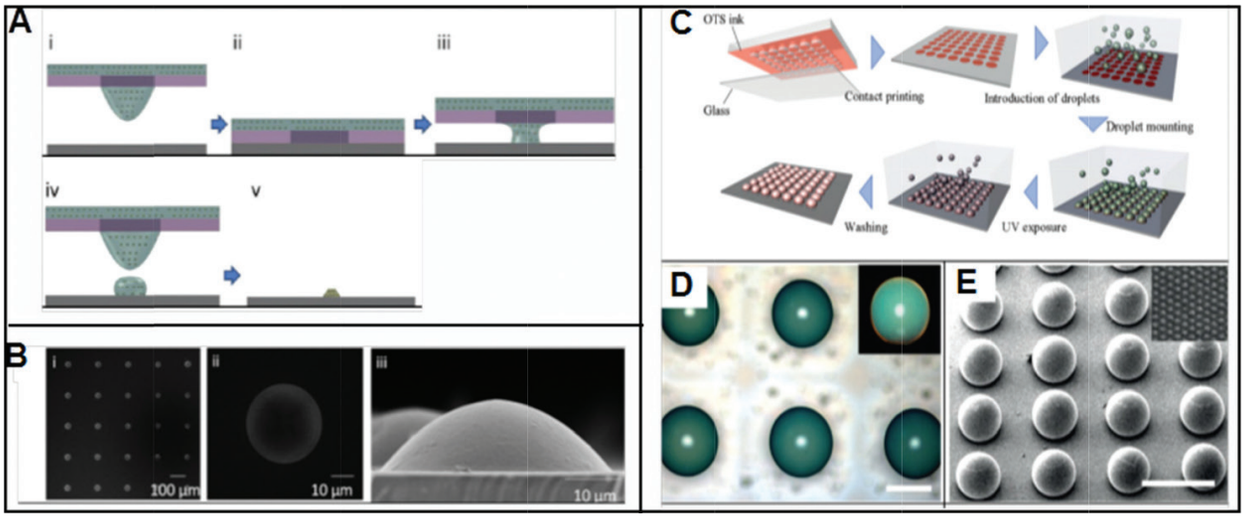

Figure 10. Schematics of printing procedure. (A) Serial processes for the fabrication of the PC sphere on hydrophobic substrate. (B) SEM views of zinc oxide nanoparticle (diameter ≈ 30 nm) clusters [44]. (C) Schematic of mounting and solidifying of droplets on a substrate pre-patterned with a hydrophobic moiety. (D) Optical microscopy images of patterned photonic domes of a 260-mm diameter with a 500-mm interval. They are composed of 170-nm silica particles (33 vol%) in an ETPTA matrix. (E) SEM image of the dome pattern; the inset shows the surface morphology of the dome. Scale bars, 500 μm [56].

The oil phase was ethoxylated trimethylolpropane triacrylate (ETPTA), which could be photocurabled. In water, a high CA of 158.4°for ETPTA on the bare glass was showed but it was inclined to spread over the OTS-coated glass with a low CA of 8°. As a result, the ETPTA drops could be selectively adsorbed on the patterned OTS dots. Finally, a pattern of hemispherical colloidal PC was prepared by using ETPTA droplets with SiO_2 particles. The as-prepared colloidal PC dome presented hexagonal arrangement of colloidal silica particles on its surface, which corresponded to the (111) plane of the FCC lattice.

Ultratrace detection is of enormous interest in early diagnosis, drugs testing, explosives detection, and ecopollution determination [57–60]. Fog collecting structure on Stenocara beetle's back gives a good example to fabricate a PC microchip with hydrophilic–hydrophobic micropattern by inkjet printing. It makes high-sensitive ultratrace detection of fluorescence analytes and fluorophore-based assays possible. For example, Hou et al. [20] prepared a PC microchip which was printed by the hydrophilic monodispersed poly(styrene-methylmethacrylate-acrylic acid) (poly(St-MMA-AA)) spheres on a hydrophobic polydimethylsiloxane (PDMS) substrate. All PC dots (**Figure 11A**) were about 200 mm in diameter. They were assembled from the monodispersed colloidal spheres with diameters of 180, 215, and 240 nm, named as PC_{180}, PC_{215}, and PC_{240}, respectively. The wettability between a PC dot and a PDMS substrate

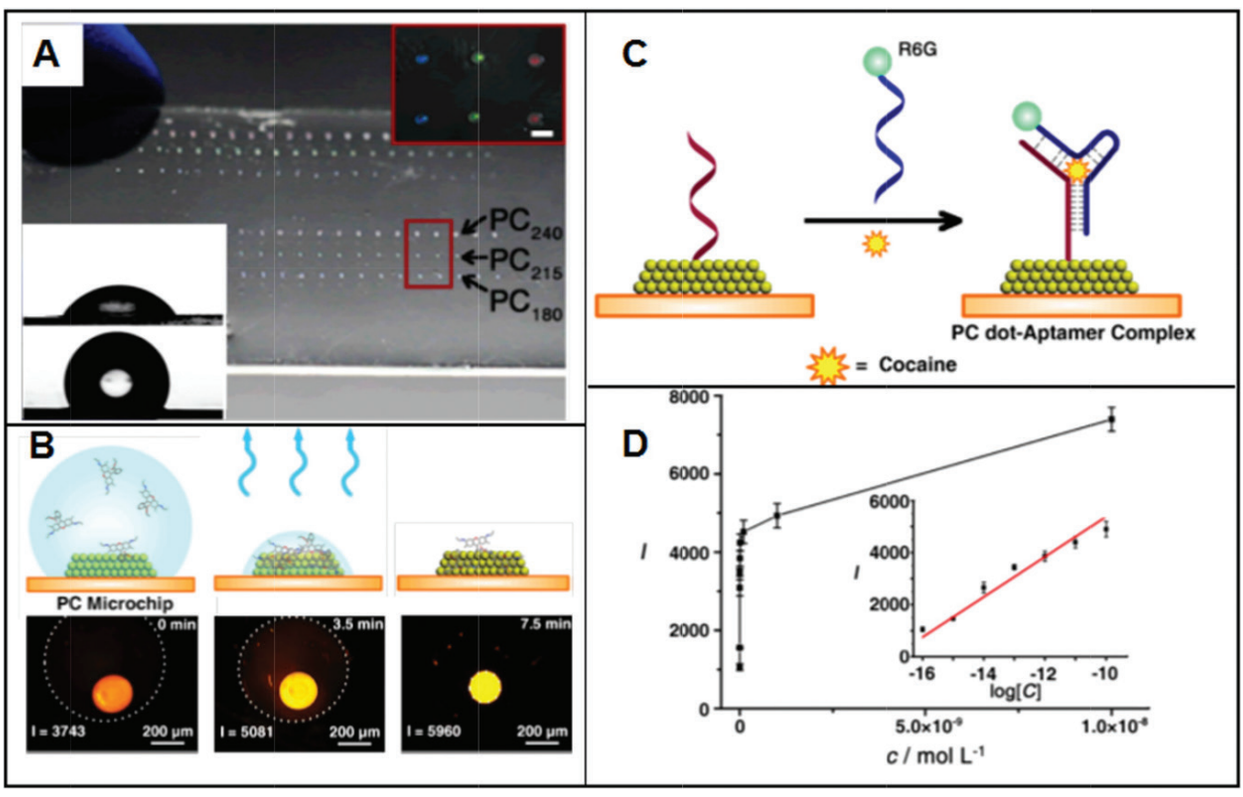

Figure 11. (A) Photography of the bio-inspired PC microchip with hydrophilic PC dots on hydrophobic substrate. The inset shows the magnified picture corresponding to PC dots of different stopbands. The scale bar is 200 mm. The CA of PDMS substrate is 115.0 ± 3.1° while CA of the PC dot was 46.4 ± 3.4°.(B) schematic representation of the cocaine detection mechanism and the fluorescence intensities at different cocaine concentrations. The inset shows a linear relationship between fluorescence intensity and the logarithm of the cocaine concentration (1×10^{-10} to 1×10^{-16} mol L^{-1}) [20].

is quite different. Because of hydrophilic-hydrophobic micropattern, the analyte in the highly diluted solution droplet can be concentrated onto the PC dot. This phenomenon is mainly due to the wettability difference between the hydrophilic PC dot and the hydrophobic PDMS substrate. The solution dewetted from the hydrophobic substrate and was concentrated to the hydrophilic PC dot with the water evaporation. In **Figure 11B**, the PC dot was functionalized with capture DNA. By enriching the cocaine molecules and the R6G-labeled target DNA from solution onto the PC dot, it was possible to detect cocaine. After enriching cocaine on the PC dot and specifically capturing by a DNA-functionalized PC dot and R6G-labeled target DNA, the high-efficient fluorescence detection could be realized (**Figure 11C** and **D**).

5. Conclusions

In conclusion, we presented a summarization about the influence of the substrate wettability on colloidal assembly. It is clear that the substrate with different wettability produces a distinct influence on the colloidal assembly process, the resultant assembly structure and the resulting functionality, it will bring about new insight for the creation of novel-type PC optic devices.

Author details

Junchao Liu, Jingxia Wang* and Lei Jiang

*Address all correspondence to: jingxiawang@mail.ipc.ac.cn

CAS, Key Laboratory of Bio-inspired Materials and Interface Sciences, Technical Institute of Physics and Chemistry Chinese Academy of Sciences, Beijing, China

References

[1] Yablonovitch E. Inhibited spontaneous emission in solid-state physics and electronics. Physical Review Letters. 1987;**58**:2059-2062. DOI: 10.1103/PhysRevLett.58.2059

[2] John S. Strong localization of photons in certain disordered dielectric superlattices. Physical Review Letters. 1987;**58**:2486-2489. DOI: 10.1103/PhysRevLett.58.2486

[3] Yablonovitch E. Photonic band-gap crystals. Journal of Physics: Condensed Matter. 1993;**5**:2443-2460. DOI: 10.1088/0953-8984/5/16/004

[4] Joannopoulos JD, Villeneuve PR, Fan SH. Photonic crystals: Putting a new twist on light. Nature. 1997;**386**:143-149. DOI: 10.1038/386143a0

[5] Fang Y, Ni YL, Leo SY, Taylor C, Basile V, Jiang P. Reconfigurable photonic crystals enabled by pressure-responsive shape-memory polymers. Nature Communications. 2015;**6**:7416. DOI: 10.1038/ncomms8416

[6] Liu JC, Wan L, Zhang MB, Jiang KJ, Song K, Wang JX, Ikeda T, Jiang L. Electrowetting-induced morphological evolution of metal-organic inverse opals toward a water-lithography approach. Advanced Functional Materials. 2017;**27**:1605221. DOI: 10.1002/adfm.201605221

[7] Burgess IB, Mishchenko L, Hatton BD, Kolle M, Loncar M, Aizenberg J. Encoding complex wettability patterns in chemically functionalized 3D photonic crystals. Journal of the American Chemical Society. 2011;**133**:12430-12432. DOI: 10.1021/ja2053013

[8] Teyssier J, Saenko SV, van der Marel D, Milinkovitch MC. Photonic crystals cause active colour change in chameleons. Nature Communications. 2015;**6**:6368. DOI: 10.1038/ncomms7368

[9] Qin M, Huang Y, Li YN, Su M, Chen BD, Sun H, Yong PY, Ye CQ, Li FY, Song YL. A rainbow structural-color Chip for multisaccharide recognition. Angewandte Chemie, International Edition. 2016;**55**:6911-6914. DOI: 10.1002/anie.201602582

[10] Sun XM, Zhang J, Lu X, Fang X, Peng HS. Mechanochromic photonic-crystal fibers based on continuous sheets of aligned carbon nanotubes. Angewandte Chemie, International Edition. 2015;**54**:3630-3634. DOI: 10.1002/anie.201412475

[11] Kuno T, Matsumura Y, Nakabayashi K, Atobe M. Electroresponsive structurally colored materials: A combination of structural and Electrochromic effects. Angewandte Chemie, International Edition. 2016;**55**:2503-2506. DOI: 10.1002/anie.201511191

[12] Yin SN, Yang SY, Wang CF, Chen S. Magnetic-directed assembly from Janus building blocks to multiplex molecular-analogue photonic crystal structures. Journal of the American Chemical Society. 2016;**138**:566-573. DOI: 10.1021/jacs.5b10039

[13] Ge JP, Yin YD. Responsive photonic crystals. Angewandte Chemie, International Edition. 2011;**50**:1492-1522. DOI: 10.1002/anie.200907091

[14] Li HL, Wang JX, Yang LM, Song YL. Superoleophilic and Superhydrophobic inverse opals for oil sensors. Advanced Functional Materials. 2008;**18**:3258-3264. DOI: 10.1002/adfm.200800507

[15] Ye XZ, Li Y, Dong JY, Xiao JY, Ma YR, Qi LM. Facile synthesis of ZnS Nanobowl arrays and their applications as 2D photonic crystal sensors. Journal of Materials Chemistry C. 2013;**1**:6112-6119. DOI: 10.1039/c3tc30118d

[16] Gur D, Palmer BA, Leshem B, Oron D, Fratzl P, Weiner S, Addadi L. The mechanism of color change in the neon tetra fish: A light-induced tunable photonic crystal Array. Angewandte Chemie, International Edition. 2015;**54**:12426-12430. DOI: 10.1002/anie.201502268

[17] Liu CH, Ding HB, ZQ W, Gao BB, FF F, Shang LR, ZZ G, Zhao YJ. Tunable structural color surfaces with visually self-reporting wettability. Advanced Functional Materials. 2016;**26**:7937-7942. DOI: 10.1002/adfm.201602935

[18] YN W, Li FT, Zhu W, Cui JC, Tao CA, Lin CX, Hannam PM, Li GT. Metal-organic frameworks with a three-dimensional ordered macroporous structure: Dynamic photonic materials. Angewandte Chemie, International Edition. 2011;**50**:12518-12522. DOI: 10.1002/anie.201104597

[19] Zhang YQ, Fu QQ, Ge JP. Photonic sensing of organic solvents through geometric study of dynamic reflection Spectrum. Nature Communications. 2015;**6**:7510. DOI: 10.1038/ncomms8510

[20] Hou J, Zhang HC, Yang Q, Li MZ, Song YL, Jiang L. Bio-inspired photonic-crystal microchip for fluorescent Ultratrace detection. Angewandte Chemie, International Edition. 2014;**53**:5791-5795. DOI: 10.1002/anie.201400686

[21] Vogel N, Belisle RA, Hatton B, Wong TS, Aizenberg J. Transparency and damage tolerance of Patternable Omniphobic lubricated surfaces based on inverse colloidal monolayers. Nature Communications. 2013;**4**:2176. DOI: 10.1038/ncomms3176

[22] Sano K, Kim YS, Ishida Y, Ebina Y, Sasaki T, Hikima T, Aida T. Photonic water dynamically responsive to external stimuli. Nature Communications. 2016;**7**:12559. DOI: 10.1038/ncomms12559

[23] Cubillas AM, Schmidt M, Euser TG, Taccardi N, Unterkofler S, Russell PS, Wasserscheid P, Etzold BJM. In situ heterogeneous catalysis monitoring in a hollow-Core photonic crystal fiber microflow reactor. Advanced Materials Interfaces. 2014;**1**:1300093. DOI: 10.1002/admi.201300093

[24] Mazingue T, Lomello TM, Hernandez RC, Passard M, Goujon L, Rousset JL, Morfin F, Bosselet F, Maulion G, Kribich R. Pellet photonic Innovant gas sensor using catalysis and integrated photonics. Sensors and Actuators B: Chemical. 2016;**222**:133-140. DOI: 10.1016/j.snb.2015.07.107

[25] Chen M, Zhang YP, Jia SY, Zhou L, Guan Y, Zhang YJ. Photonic crystals with a reversibly inducible and erasable defect state using external stimuli. Angewandte Chemie, International Edition. 2015;**54**:9257-9261. DOI: 10.1002/anie.201503004

[26] Chen K, Tuysuz H. Morphology-controlled synthesis of Organometal halide Perovskite inverse opals. Angewandte Chemie, International Edition. 2015;**54**:13806-13810. DOI: 10.1002/anie.201506367

[27] Fan J, Li YN, Bisoyi HK, Zola RS, Yang DK, Bunning TJ, Weitz DA, Li Q. Light-directing omnidirectional circularly polarized reflection from liquid-crystal droplets. Angewandte Chemie, International Edition. 2015;**54**:2160-2164. DOI: 10.1002/anie.201410788

[28] Gur D, Palmer BA, Weiner S, Addadi L. Light manipulation by guanine crystals in organisms: Biogenic Scatterers, mirrors, multilayer reflectors and photonic crystals. Advanced Functional Materials. 2017;**27**:1603514. DOI: 10.1002/adfm.201603514

[29] Lee SY, Choi JK, Jeong JR, Shin JH, Kim SH. Magnetoresponsive photonic microspheres with structural color gradient. Advanced Materials. 2017;**29**:1605450. DOI: 10.1002/adma.201605450

[30] Kim KH, Hwang MS, Kim HR, Choi JH, No YS, Park HG. Direct observation of exceptional points in coupled photonic-crystal lasers with asymmetric optical gains. Nature Communications. 2016;**7**:13893. DOI: 10.1038/ncomms13893

[31] Zhai Y, Ma YG, David SN, Zhao DL, Lou RN, Tan G, Yang RG, Yin XB. Scalable-manufactured randomized glass-polymer hybrid Metamaterial for daytime Radiative cooling. Science. 2017;**355**:1062-1066. DOI: 10.1126/science.aai7899

[32] Wu H, Kuang XH, Cui LY, Tian D, Wang MH, Luan GY, Wang JX, Jiang L. Single-material solvent-sensitive actuator from poly(ionic liquid) inverse opals based on gradient Gewetting. Chemical Communications. 2016;**52**:5924-5927. DOI: 10.1039/c6cc01442a

[33] Kralchevsky PA, Denkov ND. Capillary forces and structuring in layers of colloid particles. Current Opinion in Colloid & Interface Science. 2001;**6**:383-401. DOI: 10.1016/S1359-0294(01)00105-4

[34] Denkov ND, Velev OD, Kralchevsky PA, Ivanov IB, Yoshimura H, 2-Dimensional Crystallization NK. Nature. 1993;**361**:26-26. DOI: 10.1038/361026a0

[35] Tian Y, Jiang L. Wetting intrinsically robust hydrophobicity. Nature Materials. 2013;**12**:291-292. DOI: 10.1038/nmat3610

[36] Gu ZZ, Yu YH, Zhang H, Chen H, Lu Z, Fujishima A, Sato O. Self-assembly of Monodisperse spheres on substrates with different wettability. Applied Physics A: Materials Science & Processing. 2005;**81**:47-49. DOI: 10.1007/s00339-004-3020-4

[37] Sun ZJ, Bao B, Jiang JK, He M, Zhang XY, Song YL. Facile fabrication of a Superhydrophilic-superhydrophobic patterned surface by inkjet printing a sacrificial layer on a Superhydrophilic surface. RSC Advances. 2016;**6**:31470-31475. DOI: 10.1039/c6ra02170k

[38] Liu MJ, Wang JX, He M, Wang LB, Li FY, Jiang L, Song YL. Inkjet printing controllable footprint lines by regulating the dynamic wettability of coalescing ink droplets. ACS Applied Materials and Interfaces. 2014;**6**:13344-13348. DOI: 10.1021/am5042548

[39] Kuang MX, Wang JX, Bao B, Li FY, Wang LB, Jiang L, Song YL. Inkjet printing patterned photonic crystal domes for wide viewing-angle displays by controlling the sliding three phase contact line. Advanced Optical Materials. 2014;**2**:34-38. DOI: 10.1002/adom.201300369

[40] Cui LY, Zhang JH, Zhang XM, Li YF, Wang ZH, Gao HN, Wang TQ, Zhu SJ, HL Y, Yang B. Avoiding coffee ring structure based on hydrophobic silicon pillar arrays during single-drop evaporation. Soft Matter. 2012;**8**:10448-10456. DOI: 10.1039/c2sm26271a

[41] Kim SH, Lim JM, Jeong WC, Choi DG, Yang MY. Patterned colloidal photonic domes and balls derived from viscous Photocurable suspensions. Advanced Materials. 2008;**20**:3211-3217. DOI: 10.1002/adma.200800782

[42] Bao B, Li MZ, Li Y, Jiang KJ, ZK G, Zhang XY, Jiang L, Song YL. Patterning fluorescent quantum dot Nanocomposites by reactive inkjet printing. Small. 2015;**11**:1649-1654. DOI: 10.1002/smll.201403005

[43] Kawamura A, Kohri M, Yoshioka S, Taniguchi T, Kishikawa K. Structural color tuning: Mixing melanin-like particles with different diameters to create neutral colors. Langmuir. 2017;**33**:3824-3830. DOI: 10.1021/acs.langmuir.7b00707

[44] Choi S, Jamshidi A, Seok TJ, MC W, Zohdi TI. Fast, high-throughput creation of size-tunable micro/nanoparticle clusters via evaporative self-assembly in Picoliter-scale droplets of particle suspension. Langmuir. 2012;**28**:3102-3111. DOI: 10.1021/la204362s

[45] Ding HB, Zhu C, Tian L, Liu CH, Fu GB, Shang LR, Gu ZZ. Structural color patterns by Electrohydrodynamic jet printed photonic crystals. ACS Applied Materials and Interfaces. 2017;**9**:11933-11941. DOI: 10.1021/acsami.6b11409

[46] Qin M, Huang Y, Li YN, Su M, Chen BD, Sun H, Yang PY, Yang CQ, Li FY, Song YL. A rainbow structural-color Chip for multisaccharide recognition. Angewandte Chemie, International Edition. 2016;**55**:6911-6914. DOI: 10.1002/anie.201602582

[47] Rastogi V, Melle S, Calderón OG, GarcÍa AA, Marquez M, Velev OD. Synthesis of light-diffracting assemblies from microspheres and nanoparticles in droplets on a Superhydrophobic surface. Advanced Materials. 2008;**20**:4263-4268. DOI: 10.1002/adma.200703008

[48] Rastogi V, GarcÍa AA, Marquez M, Velev OD. Anisotropic particle synthesis inside droplet templates on Superhydrophobic surfaces. Macromolecular Rapid Communications. 2010;**31**:190-195. DOI: 10.1002/marc.200900587

[49] Zhou JM, Yang J, Gu ZD, Zhang GF, Wei Y, Yao X, Song YL, Jiang L. Controllable fabrication of noniridescent microshaped photonic crystal assemblies by dynamic three-phase contact line behaviors on Superhydrophobic substrates. ACS Applied Materials and Interfaces. 2015;**7**:22644-22651. DOI: 10.1021/acsami.5b07443

[50] Huang Y, Zhou JM, Su B, Shi L, Wang JX, Chen SR, Wang LB, Zi J, Song YL, Jiang L. Colloidal photonic crystals with narrow Stopbands assembled from low-adhesive Superhydrophobic substrates. Journal of the American Chemical Society. 2012;**134**:17053-17058. DOI: 10.1021/ja304751k

[51] Gu ZZ, Fujishima A, Sato O. Patterning of a colloidal crystal film on a modified hydrophilic and hydrophobic surface. Angewandte Chemie, International Edition. 2002;**4**:2068-2070. DOI: 10.1002/1521-3757

[52] Lee SW, Na YJ, Choi Y, Lee SD. Site-selective assembly and fixation of colloidal particles into two-dimensional Array on wettability-patterned surface. Japanese Journal of Applied Physics. 2007;**46**:1129-1131. DOI: 10.1143/JJAP.46.L1129

[53] Wu L, Dong ZC, Kuang MX, Li YN, Li YF, Jiang L, Song YL. Printing patterned fine 3D structures by manipulating the three phase contact line. Advanced Functional Materials. 2015;**25**:2237-2242. DOI: 10.1002/adfm.201404559

[54] Wang YZ, Wei C, Cong HL, Yang Q, Wu YC, Su B, Zhao YS, Wang JX, Jiang L. Hybrid top-down/bottom-up strategy using Superwettability for the fabrication of patterned colloidal assembly. ACS Applied Materials and Interfaces. 2016;**8**:4985-4993. DOI: 10.1021/acsami.5b11945

[55] Yoo JH, Kwon HJ, Paeng D, Yeo J, Elhadj S, Grigoropoulos CP. Facile fabrication of a superhydrophobic cage by laser direct writing for site-specific colloidal self-assembled photonic crystal. Nanotechnology. 2016;**27**:145604. DOI: 10.1088/0957-4484/27/14/145604

[56] Kim SH, Kim SH, Yang SM. Patterned polymeric domes with 3D and 2D embedded colloidal crystals using Photocurable emulsion droplets. Advanced Materials. 2009;**21**: 3771-3775. DOI: 10.1002/adma.200901243

[57] Arya SK, Bhansali S. Lung cancer and its early detection using biomarker-based biosensors. Chemical Reviews. 2011;**111**:6783-6809. DOI: 10.1021/cr100420s

[58] Apple FS, Smith SW, Pearce LA, Ler R, Murakami MM. Use of the centaur TnI-ultra assay for Ddetection of myocardial infarction and adverse events in patients presenting with symptoms suggestive of acute coronary syndrome. Clinical Chemistry. 2008;**54**:723-728. DOI: 10.1373/clinchem.2007.097162

[59] Steinfeld JI, Wormhoudt J. Explosives detection: A challenge for physical chemistry. Annual Review of Physical Chemistry. 1998;**49**:203-232. DOI: 10.1146/annurev.physchem.49.1.203

[60] Zhang HX, Hu JS, Yan CJ, Jiang L, Wan L. Functionalized carbon nanotubes as sensitive materials for electrochemical detection of ultra-trace 2,4,6-trinitrotoluene. Physical Chemistry Chemical Physics. 2006;**8**:3567-3572. DOI: 10.1039/b604587c